

Growth of Cadmium Hexacyanidoferrate(III) Nanocubes and Its Application in Voltammetric Determination of Morphine

Shah Raj Ali,*[1] Prakash Chandra,[1] Mamta Latwal,[1] Shalabh Kumar Jain,[2] and Vipin Kumar Bansal[3]

[1]Department of Chemistry, Kumaun University, Nainital 263 002, Uttarakhand, India

[2]Department of Chemistry, Gurukula Kangri University, Haridwar 249 404, Uttarakhand, India

[3]Faculty of Chemistry, Department of Applied Science, Mangalayatan University, Aligarh 202 145, Uttar Pradesh, India

Received April 25, 2011; E-mail: shahrajali@gmail.com

Cadmium hexacyanidoferrate(III) nanocubes (CdFeNc) have been synthesized and characterized using elemental analysis, thermal analysis, infrared spectroscopy, and X-ray diffraction technique. FE-SEM image showed that nanoparticles have cubic shape with size range 60–90 nm. Electrochemical behavior of CdFeNc has been studied. Electrocatalytic oxidation of morphine was studied using a cadmium hexacyanidoferrate(III) nanocube–carbon nanotube composite modified glassy carbon electrode (CdFeNc–CNT/GCE). The modified electrode reduced the peak potential of morphine by nearly 95 mV. The CdFeNc–CNT/GCE showed a linear response in a concentration range of 500–20 μM. The correlation coefficients (R) for phenolic and t-amine groups of morphine were 0.9925 and 0.9996 respectively while their sensitivity was 3.363 and 4.154 $\mu A\,\mu M^{-1}$. The CdFeNc–CNT/GCE exhibited a detection limit of 0.21 μM for phenolic and t-amine groups of morphine.

Due to their extraordinary size and shape dependent properties nanomaterials show potential applications in various interdisciplinary areas viz., biological diagnosis, biomedicine, controlled drug delivery, enzyme immobilization, magnetic resonance imaging, and magnetic memory devices. Besides the above, nanomaterials have made a big impact in the development of voltammetric sensors for many pharmaceutically and biologically important molecules. The development of nanomaterial-based sensors is a subject of growing interest due to their extreme simplicity, short analysis time, low cost, high sensitivity, and specificity as compared to other techniques such as GC-MS, HPLC, TLC, electrophoresis, and spectrophotometery. In this context, the excellent redox mediator properties and other outstanding characteristics of metal hexacyanidoferrates(III) open a new frontier for the development of voltammetric sensors. These materials exhibit mixed valency, high ionic conductivity, excellent magnetic properties, counteraction storage ability, and capability to mediate electrochemical reactions.[1–4] Most of these complexes possess microporous, polynuclear, and open channel structure.[5–7] These materials do not dissolve during their oxidation/reduction as their zeolitic structure allows the diffusion of ions toward the inside or outside to maintain electrical charge neutrality. Due to all the above properties, metal hexacyanidoferrates(III) have been used for electrochemical detection of several biomolecules. Yang et al. reported a carbon nanotube–cobalt hexacyanidoferrate(III) nanoparticles-based sensor for glucose.[8] Cui et al. reported a copper–cobalt hexacyanidoferrate-modified electrode for hydrogen peroxide sensing.[9] A cobalt hexacyanidoferrate(III) nanotube-modified electrode for electrochemical determination of ascorbic acid and dopamine has been reported by Shi et al.[10] Chen and Peng reported cobalt hexacyanidoferrates(III)-modified electrodes for sensing of dopamine, epinephrine, and norepinephrine.[11] Electrochemical determination of β-NADPH using a copper hexacyanidoferrate-modified electrode has been developed by Chen and Chan.[12] Qu et al. reported a cobalt hexacyanidoferrates(III)–CNT-modified electrode for insulin sensing.[13] Electrochemical determination of paracetamol using a cobalt hexacyanidoferrate-modified electrode has been reported by Prabakar and Narayanan.[14] Razmi and Taghvimi developed a hydrogen peroxide biosensor using a tin hexacyanidoferrate-modified electrode.[15] Eftekhari studied the electrochemical behavior of a zinc hexacyanidoferrate film-modified electrode.[16] Heli et al. studied charge propagation in nanoparticles of Fe_2O_3 core–cobalt hexacyanidoferrates using electrochemical impedance spectroscopy.[17] Prabhu et al. reported nickel hexacyanidoferrate-modified electrodes for amperometric determination of L-dopa.[18] Boopathi et al. studied the selective deposition of zinc hexacyanidoferrates on metal impurity sites of SWCNT/glassy carbon electrodes.[19] Electrochemical behavior of metal hexacyanidocobaltates has been studied by Kasem et al.[20] Bustos and Godinez studied a nanostructured Prussian blue-modified electrode for their advanced electrochemical applications.[21] An electrochromic device has been developed using a zinc hexacyanidoferrate(III)/PEDOT:PSS composite counter electrode.[22] Recently, a cobalt hexacyanidoferrate(III) graphite wax composite electrode has been used for the amperometric determination of morphine.[23] In most cases, metal hexacyanidoferrates(III) were utilized in their conventional form as their nanochemistry has not been well studied so far. However, little work has been published on the synthesis of metal hexacyanidoferrate(III) nanoparticles.[24–30] We are interested in synthesizing the nanoparticles of transition-metal hexacyanidoferrates(III) and to explore their catalytic and electrocatalytic activities. Recently, we have reported the growth of zinc hexacyanidoferrate(II) nanocubes and their

Published on the web December 6, 2011; doi:10.1246/bcsj.20110117

catalytic application.[31] In this paper, we have described the growth of CdFeNc and its electrocatalytic application in voltammetric determination of morphine using CdFeNc–CNT/GCE. The voltammetric determination of morphine is an important issue as it belongs to a group of most abused drugs and causes several adverse effects on human health when given in overdose. It is frequently used as a potent narcotic analgesic drug to relieve severe pain, especially for those undergoing a surgical procedure and moderate cancer-related pain. Researchers have reported voltammetric sensors for morphine in plasma, urine, and opium samples.[32–34]

Experimental

Chemicals. $K_3[Fe(CN)_6]\cdot H_2O$, $Cd(NO_3)_2\cdot 6H_2O$, KCl, KNO_3, and EDTA were purchased from Merck. Aldrich manufactured morphine was used without further purification. All other chemicals of analytical reagent grade and doubly distilled water were used.

Synthesis of CdFeNc. CdFeNc were synthesized from $K_3[Fe(CN)_6]\cdot H_2O$ using a reported method.[13] It involved dropwise slow addition of 50 mL of 0.01 M $Cd(NO_3)_2\cdot 6H_2O$ solution containing an equimolar amount of EDTA into a 25 mL of 0.01 M $K_3[Fe(CN)_6]\cdot H_2O$ solution containing an equimolar amount of KCl with constant stirring at room temperature. After complete mixing of solutions, the reaction mixture was vigorously agitated for 5 min and then kept undisturbed for 30 min. The aqueous suspension so obtained was filtered, washed thoroughly with water, and dried in an air oven at 60 °C overnight. It was crushed and sieved with a 100 mesh.

Characterization of CdFeNc. The percentage of C, H, and N was recorded on an Elementar Vario EL-III CHNS analyzer. The percentage of Cd and Fe was recorded on a Perkin-Elmer atomic absorption spectrophotometer. The TG/DT analysis was carried out using a Perkin-Elmer analyzer system (Pyris Diamond). The heating rate was 10 °C min^{-1} and all the measurements were performed in air atmosphere using Al_2O_3 as reference. The IR spectrum was recorded in KBr film using a Perkin-Elmer Spectrophotometer. The X-ray diffraction pattern was recorded using a Philips PW-1140/90 X-ray diffractometer. The surface morphology and particle size of the synthesized material was analyzed using a Quanta 200 FE-SEM instrument. The surface area was determined using BET method which involves the physical adsorption of N_2 at its boiling temperature.

Modification of Electrode. 4 mg of CdFeNc was dispersed in 4 mL acetone (1 mg mL^{-1}) and approximately 3 μL of it was cast on a unit area of GCE surface (3 mm diameter). The vaporization of acetone produced a thin and robust film of CdFeNc on GCE. Similarly, CdFeNc and CNT (single walled) in their different ratio (4:1, 4:2, 4:3, 4:4, and 4:5) were dispersed in acetone (1 mg mL^{-1}) and 3 μL of the suspension was cast on a unit area of GCE. These ratios of CdFeNc and CNT were controlled by increasing the amount of CNT from 1 to 5 mg keeping the amount of CdFeNc fixed (4 mg). The CdFeNc/GCE and CdFeNc–CNT/GCE so prepared were then rinsed thoroughly with distilled water and used for electrochemical studies.

Electrochemical Measurements. The electrochemical experiments were carried out using a cyclic voltammeter (Paras Industrial Products Roorkee, India). A conventional electrochemical cell consisting of three electrodes, namely, Pt wire as counter electrode, Ag/AgCl as reference electrode, and modified GCE as working electrode was used. All electrochemical measurements were carried out at 25 ± 0.2 °C. A 0.1 M $KNO_3 + 2.5 \times 10^{-2}$ M phosphate buffer solution (7.0 pH) was employed for the electrocatalytic oxidation of morphine. N_2 gas was passed through the solutions for 15 min before their use in electrochemical measurements.

Results and Discussion

Synthesis of CdFeNc. The mixing of a solution of Cd^{2+} in a solution of $[Fe(CN)_6]^{3-}$ under reaction conditions used herein results into the growth of CdFeNc. The EDTA added during the course of reaction probably facilitates the formation of CdFeNc of a uniform shape. Qu et al. has suggested the same function of EDTA for the synthesis of cobalt hexacyanidoferrate(III) nanoparticles.[13] Ocaña et al. reported that the complexation of Co^{2+} with EDTA decreases the effective concentration of Co^{2+}, which results in homogeneous precipitation of cobalt hexacyanidoferrate(III) nanoparticles.[29] The composition of synthesized material was determined by CHNS analysis, atomic absorption spectroscopy, and TG/DT analysis. The results of elemental analysis and TG/DT analysis are shown in Table 1. The TG/DT curve is shown in Figure 1a. It exhibits 22.10% mass loss up to 164 °C. This mass loss corresponded to the decomposition of water content in the synthesized material. It has been reported that the metal hexacyanidoferrates(III) liberate only water molecules on thermal decomposition up to 165 °C.[6] Table 1 shows that the observed elemental percentage and percent mass loss are nearly the same as the theoretical values calculated for $Cd_3[Fe(CN)_6]_2\cdot 12H_2O$. The synthesized material was examined by X-ray diffraction measurements and the results are shown in Table 2. The IR spectrum of the synthesized cadmium hexacyanidoferrate(III) showed a strong peak at 2068 cm^{-1} for the characteristic peak of C≡N group present in –Fe(III)–CN–Cd(II)– units. The IR spectrum showed a prompt peak at 1633 cm^{-1} for Fe–C stretching. A broad band at 3453 cm^{-1} for H–O groups of water present in the interstitial sites was also observed in the infrared spectrum. The FE-SEM image of the synthesized material is shown in Figure 1b. It showed that the synthesized material consists of well defined cubic particles with size ranging from 60 to 90 nm. Its morphology was clear and well dispersed with nanocubes. However, slightly agglomerated nanocubes were also seen in FE-SEM images. Surface area of the synthesized material was found to be 17.57 $m^2\,g^{-1}$.

Hexacyanidoferrates(III) of divalent transition-metal ions have a general molecular formula $M_3[Fe(CN)_6]_2\cdot nH_2O$, where M represents a transition metal and *n* represents the number of water molecules present in the interstitial site of the lattice.[35] The species $[Fe(CN)_6]^{3-}$ in cadmium hexacyanidoferrate(III) exist in octahedral geometry where the central Fe^{3+} ion is surrounded by six CN^- and has the electronic configuration t_{2g}.[6] Although the CN^- is bonded with Fe^{3+} through σ donation, there is

Table 1. Elemental Analyses and TG/DTA Analyses of CdFeNc

	C/%	N/%	H/%	Cd/%	Fe/%	H_2O/%
Theoretical values	14.75	17.20	2.45	34.52	11.44	22.11
Observed values	14.34	17.37	2.86	35.63	11.03	22.10

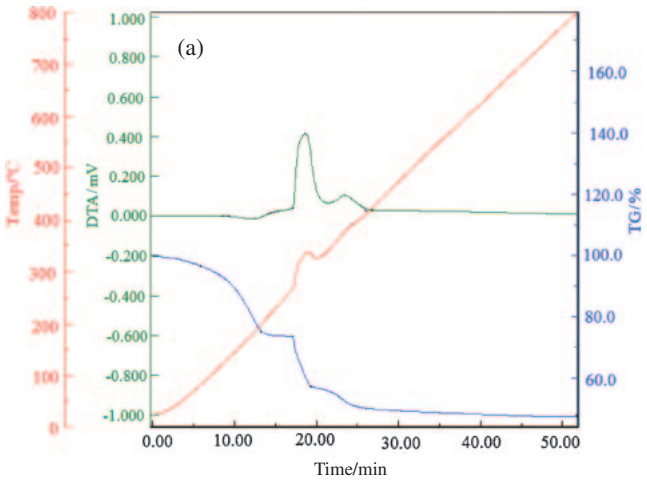

Figure 1. (a) Thermogram for TG/DT of CdFeNc. (b) FE-SEM image of CdFeNc.

Table 2. X-ray Diffraction Data of CdFeNc

S. No.	d/Å	$I/I°$
1	6.213	38
2	5.370	100
3	3.791	75
4	3.230	25
5	2.678	50
6	2.394	50
7	2.185	17
8	2.060	8s
9	1.891	17
10	1.783	17
11	1.691	13

sufficient back bonding from dπ orbitals of Fe to antibonding pπ orbitals of CN^-. In structural aspects, Prussian blue is one of the most studied metal hexacyanidoferrate(III). The face-centered cubic lattice structure of Prussian blue is the characteristic of many other transition-metal hexacyanidoferrates(III). Shriver has studied the systematics of the lattice parameters for Prussian blue analogs.[36] The transition-metal hexacyanidoferrates(III) generally have polymeric lattice structure with repetition of $[Fe(CN)_6]^{3-}$ anions, in which outer Cd^{2+} ions are coordinated with nitrogen atoms of CN^-. Detailed structural study of Prussian blue and related complexes was carried out by Ludi and Güdel.[37] Recently, Avila et al. described the atomic packing, metal coordination environment within unit cell, and structural characteristics of some metal hexacyanidoferrates(III).[6]

Characterization of CdFeNc/GCE. The cyclic voltammograms of CdFeNc/GCE were recorded in 0.1 M KNO_3 solution at different scan rates (20, 40, 60, 80, and 100 mV s^{-1}). The voltammograms are shown in Figure 2A. Each voltammogram shows the formation of a reversible redox couple. The formal potential of redox couple at scan rate of 20 mV s^{-1} was found to be 0.335 V. On increasing the scan rate, peak potential was found to shift slightly toward the negative direction. The formal potential ($E°$) and potential difference (ΔE) between anodic and cathodic peak potentials (E_a and E_c) at different scan rate were determined and the results are shown in Table 3. The formation of redox couple can be explained on the basis of redox process associated with electrochemical interconversion of $Cd^{II}[Fe^{III}(CN)_6]/Cd^{II}[Fe^{II}(CN)_6]$ as shown below:

$$Cd_3{}^{II}[Fe^{III}(CN)_6]_2 + 2e^- + 2K^+ \rightarrow K_2Cd_3{}^{II}[Fe^{II}(CN)_6]_2 \quad (1)$$

$K_2Cd_3{}^{II}[Fe^{II}(CN)_6]_2$ stands for a combined form of $Cd_2{}^{II}[Fe^{II}(CN)_6]$ and $K_2Cd^{II}[Fe^{II}(CN)_6]$. In the above redox process, one K^+ is inserted into CdFeNc when Fe^{III} gains an electron. It has been reported that the counter cations get inserted into metal hexacyanidoferrate(III) during reduction/oxidation and maintain electrical charge neutrality.[38]

The effect of different alkali metal ions in electrolyte solution was studied. For this purpose, voltammograms of CdFeNc/GCE were recorded in 0.1 M $LiNO_3$, 0.1 M $NaNO_3$, and 0.1 M KNO_3 solutions at a scan rate of 50 mV s^{-1}. The results are shown in Figure 2B. It shows a well-defined pair of redox peaks in the case of 0.1 M KNO_3 only. In cases of 0.1 M $LiNO_3$ and 0.1 M $NaNO_3$, the pair of redox peaks was broad and low. It indicates a significant decrease in peak current on substituting K^+ by Na^+ or Li^+. It also shows that the redox couple slightly shifts toward positive direction on substituting K^+ by Na^+ or Li^+. The values of E_a, E_c, $E°$, and ΔE for all the three electrolytes have been shown in Table 4. In aqueous solution, alkali metal ions exist in hydrated form and they must undergo dehydration before their insertion into crystals of metal hexacyanidoferrate(III). The electrochemical behavior of metal hexacyanidoferrates(III) in the above electrolytes may be dependent upon the ease of dehydration of hydrated alkali metal ions. The hydration energy of Li^+, Na^+, and K^+ has been reported as 5.07, 4.08, and 3.34 mV, respectively.[39] It reveals that hydrated K^+ undergoes dehydration most easily and therefore, K^+ exhibits maximum selectivity for its insertion into the cavities of CdFeNc.

The influence of concentration of KNO_3 was also studied. The voltammograms of CdFeNc/GCE were recorded in 0.5 M KNO_3, 0.10 M KNO_3, and 0.05 M KNO_3 solution at scan rate 50 mV s^{-1}. The results are shown in Figure 2C. It indicates that the redox peaks shift toward positive direction on increasing KNO_3 concentration from 0.05 to 0.5 M. The values of E_a, E_c, $E°$, and ΔE at different concentrations of KNO_3 solution are shown in Table 5. The voltammograms of CdFeNc/GCE in 0.1 M KNO_3 solution were recorded at 50 mV s^{-1} for 10 days and the results are shown in Table 6.

Effect of CNT. The effect of CNT on electrochemical behavior of CdFeNc was studied by comparing the voltammograms of CdFeNc/GCE, CNT/GCE, and CdFeNc–CNT/GCE recorded in 0.1 M KNO_3 at scan rate 50 mV s^{-1}. Figure 2D

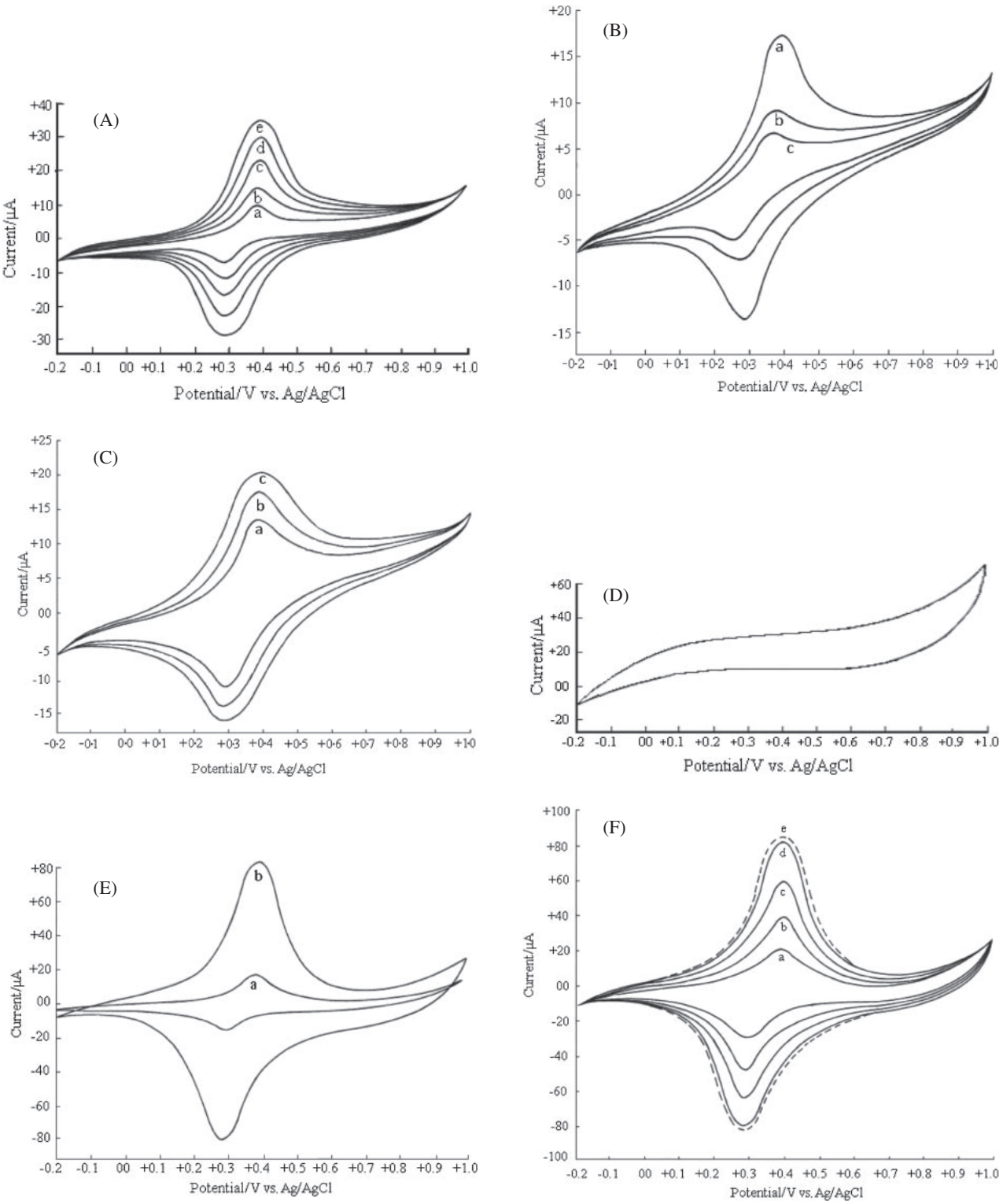

Figure 2. (A) Cyclic voltammograms of CdFeNc/GCE in 0.1 M KNO_3 at scan rate: (a) 20, (b) 40, (c) 60, (d) 80, and (e) 100 mV s^{-1}. (B) Cyclic voltammograms of CdFeNc/GCE at scan rate 50 mV s^{-1} in: (a) 0.1 M KNO_3, (b) 0.1 M $NaNO_3$, and (c) 0.1 M $LiNO_3$. (C) Cyclic voltammograms of CdFeNc/GCE at scan rate 50 mV s^{-1} in: (a) 0.05 M KNO_3, (b) 0.1 M KNO_3, and (c) 0.5 M KNO_3. (D) Cyclic voltammogram of CNT/GCE in 0.1 M KNO_3 at scan rate 50 mV s^{-1}. (E) Cyclic voltammograms of (a) CdFeNc/GCE and (b) CdFeNc–CNT/GCE in 0.1 M KNO_3 at scan rate 50 mV s^{-1}. (F) Cyclic voltammograms of CdFeNc–CNT/GCE in 0.1 M KNO_3 at scan rates 50 mV s^{-1} using CdFeNc to CNT ratio: (a) 4:1, (b) 4:2, (c) 4:3, (d) 4:4, and (e) 4:5.

shows the voltammogram of CNT/GCE. Figure 2E shows the voltammograms of CdFeNc/GCE and CdFeNc–CNT/GCE. The voltammograms of CdFeNc/GCE and CdFeNc–CNT/GCE exhibited a redox couple at peak potential of 0.34 V. It indicates that CNT did not affect the peak potential for interconversion of $Cd^{II}[Fe^{III}(CN)_6]/Cd^{II}[Fe^{II}(CN)_6]$. However, these voltammograms indicate that the peak current for CdFeNc–CNT/GCE was nearly five times more than that of CdFeNc/GCE. It showed a synergic effect in CdFeNc–CNT composite film which may be associated with the well-known excellent electron-transfer property of CNT. Figure 2F shows the voltammograms of CdFeNc–CNT/GCE recorded by changing the amount of CNT keeping the amount of CdFeNc constant in 0.1 M KNO_3 at 50 mV s^{-1}. For the purpose of analytical application, modification of GCE was carried out with composite having equal amount of CdFeNc and CNT.

Electrocatalytic Oxidation of Morphine. Electrocatalytic oxidation of morphine at CdFeNc–CNT/GCE was carried out in 0.1 M $KNO_3 + 2.5 \times 10^{-2}$ M phosphate buffer solution (7.0 pH). The voltammogram of CdFeNc–CNT/GCE was recorded in the above buffered solution at a scan rate 20 mV s^{-1} and it was found almost similar to that of the outer voltammogram of Figure 2E. This observation indicated that the addition of 2.5×10^{-2} M phosphate buffer into 0.1 M KNO_3 did not significantly affect the peak potential of CdFeNc–CNT/GCE. Now, 20 μM morphine was introduced in above solution and the voltammograms were recorded using bare GCE as well as CdFeNc–CNT/GCE. As shown in Figure 3A, the voltammogram of morphine at bare GCE gives a very weak oxidation peak at nearly 520 mV. The voltammogram of morphine at CdFeNc–CNT/GCE showed two well-defined anodic peaks in addition to that of Fe^{III}/Fe^{II}. These anodic peaks appeared at nearly 425 and 870 mV. It seems that the peaks at nearly 425 and 520 mV using CdFeNc–CNT/GCE and bare GCE, respectively, were attributed to the oxidation of the phenolic group of morphine.[40] It indicates that the CdFeNc–CNT/GCE reduces the oxidation potential of morphine by nearly 95 mV. The CdFeNc–CNT/GCE exhibited a significant increase in oxidation peak current as compared to that of bare electrode. These results show good electrocatalytic behavior of CdFeNc–CNT/GCE. Other oxidation peak observed at 870 mV may be attributed to oxidation of the *t*-amine group of morphine. The oxidation peaks for oxidation of the *t*-amine group of morphine appears at higher potential than that of its phenolic group.[40] It has been reported that oxidation of phenolic and *t*-amine substituents of morphine gives pseudomorphine and normorphine, respectively.[40] It seems that the electrocatalytic oxidation of morphine took place on the film of CdFeNc–CNT composite. It did not diffuse through the film and thus did not reach the surface of GCE. It is evident from the fact that the voltammogram of morphine at CdFeNc–CNT/GCE did not exhibit the oxidation peak at 520 mV. If morphine would have diffused through the film of CdFeNc–CNT composite and reached to the GCE surface, it must undergo electrooxidation at GCE surface and therefore it must exhibit an oxidation peak at nearly 520 mV. The electrocatalytic oxidation of morphine was carried out over a wide pH range and the peak potentials for morphine oxidation at different pH range (3.0–9.0) were recorded. The peak potential of both the anodic peaks was plotted against pH and the results are shown in Figure 3B. It showed that the peak potential increased linearly on increasing the pH from 3.0 to 9.0. It indicates that the morphine oxidation was a pH dependent process.

Calibration Plot. The voltammograms of CdFeNc–CNT/GCE were recorded over a wide concentration range of morphine (1.0×10^{-6} to 2.0×10^{-5} M) in 0.1 M $KNO_3 + 2.5 \times 10^{-2}$ M phosphate buffer solution and the results are shown in Figure 3C. The values of peak current for both the anodic peaks (at different concentration of morphine) were plotted against the morphine concentrations and the results are shown in Figure 3D. It indicates that the peak current of both

Table 3. $E°$, E_{pa}, E_{pc}, and ΔE for CdFeNc/GCE in 0.01 M KNO_3 at Different Scan Rate

S. No.	Scan rate /mV s^{-1}	E_{pa} /mV	E_{pc} /mV	$E°$ /mV	ΔE /mV
1	20	375	295	335	80
2	40	380	290	335	90
3	60	389	282	335.5	107
4	80	396	275	335.5	121
5	100	402	268	335	134

Table 4. $E°$, E_{pa}, E_{pc}, and ΔE for CdFeNc/GCE in Different Electrolyte at Scan Rate of 50 mV s^{-1}

S. No.	Electrolyte (0.1 M)	E_{pa} /mV	E_{pc} /mV	$E°$ /mV	ΔE /mV
1	KNO_3	384	286	335	98
2	$NaNO_3$	373	264	318.5	109
3	Li NO_3	368	256	312	112

Table 5. $E°$, E_{pa}, E_{pc}, and ΔE for CdFeNc/GCE in Different Concentration of KNO_3 at Scan Rate of 50 mV s^{-1}

S. No.	KNO_3 Conc. /M	E_{pa} /mV	E_{pc} /mV	$E°$ /mV	ΔE /mV
1	0.02	376	273	324.5	103
2	0.1	384	286	335	98
3	0.5	394	302	348	92

Table 6. Repeated Scan Data of CdFeNc/GCE in 0.1 M KNO_3 at Different Time and 50 mV s^{-1}

	Time/day									
	1	2	3	4	5	6	7	8	9	10
E_{pa}/mV	384	383	384	384	383	383	384	383	383	382
E_{ca}/mV	286	285	286	286	285	285	286	285	285	284
$E°$/mV	335	334	335	335	334	334	335	334	334	333
i_{pa}/μA	17.5	17.4	17.4	17.5	17.5	17.5	17.6	17.5	17.4	17.2
i_{ca}/μA	−13.4	−13.5	−13.6	−13.5	−13.5	−13.4	−13.5	−13.5	−13.6	−13.1

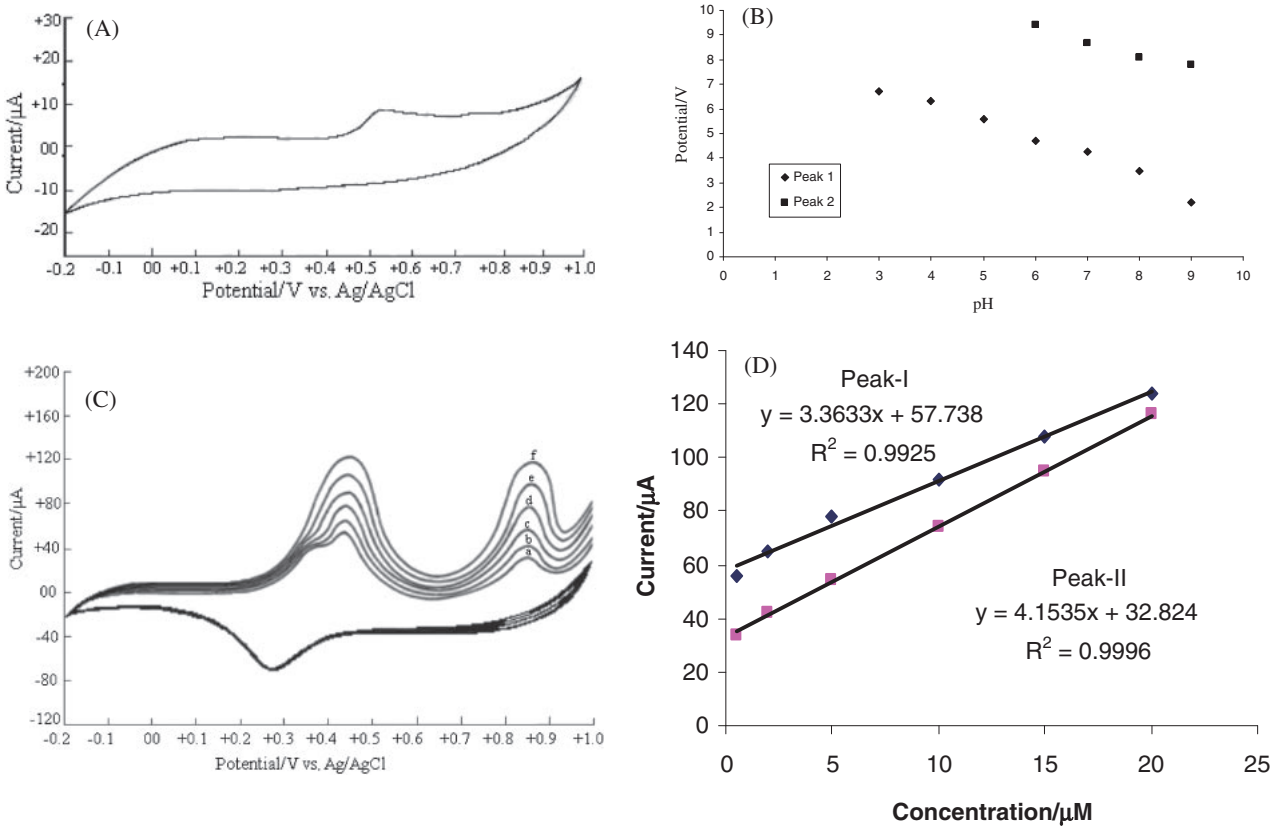

Figure 3. (A) Cyclic voltammogram of bare GCE in 0.1 M $KNO_3 + 2.5 \times 10^{-2}$ M phosphate buffer containing 20 μM morphine at scan rate 50 mV s^{-1}. (B) Plot of peak potential of morphine versus pH. (C) Cyclic voltammograms of CdFeNc–CNT/GCE in 0.1 M $KNO_3 + 2.5 \times 10^{-2}$ M phosphate buffer solution at scan rate 50 mV s^{-1} with morphine concentration: (a) 1.0×10^{-6}, (b) 4.0×10^{-6}, (c) 8.0×10^{-6}, (d) 1.2×10^{-5}, (e) 1.6×10^{-5}, and (f) 2.0×10^{-5} M. (D) The plot for peak current versus concentration of morphine.

the anodic peaks increased linearly on increasing the morphine concentration from 1.0×10^{-6} to 2.0×10^{-5} M. However, further increase in morphine concentration gave a plateau. The linear plot exhibited a correlation coefficient of 0.9925 and 0.9996 ($n = 6$) for first and second anodic peaks, respectively. The first and second anodic peaks showed sensitivity of 3.363 and 4.154 μA μM^{-1} respectively. The CdFeNc–CNT/GCE showed a detection limit of 0.21 μM for phenolic and *t*-amine groups of morphine. The stability of CdFeNc–CNT/GCE for its electrocatalytic potential for morphine was studied and it was found that there was no significant loss in electrocatalytic activity of CdFeNc–CNT/GCE up to 10 days. However, after 15 days its response current was 80% of the initial response for 2.0×10^{-5} M morphine. These results reveal a good electrocatalytic behavior of CdFeNc–CNT/GCE for morphine oxidation. It may be associated with the high redox mediator ability of CdFeNc–CNT/GCE composite film.

Analytical Utility. The CdFeNc–CNT/GCE was also examined for real sample analysis in human urine samples. The recovery of morphine was evaluated by comparing the peak current of morphine obtained from the spiked urine sample with peak current of morphine solution of the same standard concentration ($n = 5$). The results are shown in Table 7. It shows the recovery of the spiked samples to vary from 95.1% to 106.6% with RSD ($n = 5$) values of 6.4%. The response of the proposed method has been compared with some other reported methods.[40–46] The comparative data are shown in Table 8. It shows that the proposed method is more adventurous than the reported amperometric method as the proposed method can be employed for urine sample.

Table 7. Determination of Morphine in Urine Sample

Urine sample	Spiked morphine /mol L^{-1}	Recorded morphine /mol L^{-1}	Recovery /%	RSD /%[a)]
1	5.0	4.68	93.6	3.3
2	10.0	10.60	106	4.6
3	15.0	14.54	96.3	6.7

a) Average of five replicate measurements.

Conclusion

CdFeNc can be synthesized by mixing of a solution of Cd^{2+} into a solution of $[Fe(CN)_6]^{3-}$ under reaction conditions used herein and EDTA controls the uniform shape of CdFeNc. CdFeNc–CNT/GCE shows good electrocatalytic activities for oxidation of morphine. The correlation coefficients (R) for first and second oxidation peaks of morphine were 0.9925 and 0.9996, respectively, while their sensitivity was 3.363 and 4.154 μA μM^{-1}. The CdFeNc–CNT/GCE exhibited a detection limit of 0.21 phenolic and *t*-amine groups of morphine. The CdFeNc–CNT/GCE exhibited good performance and can be used for analysis of morphine in human urine samples.

Table 8. Comparison of Results of Proposed Method with Some Reported Methods

Method	Sample	Detection limit	Recovery/%	Reference
Microchip CE[a)]	Urine	$0.2\,\mu M\,L^{-1}$	96.2	40
LPME[b)]–HPLC[c)]	Urine	$0.05\,mg\,L^{-1}$	92.4–106.8	41
Amperometry	Not applied	$0.2\,mM\,L^{-1}$	—	42
Amperometry-MIP[d)]	Not applied	$0.3\,mM\,L^{-1}$	—	43
SIA[e)]	Urine	$0.076\,\mu g\,L^{-1}$	96.3	44
DPV[f)]	Plasma	$0.01\,\mu M\,L^{-1}$	98.5–102.5	45
Amperometry	Not applied	$0.2\,\mu M\,L^{-1}$	—	46
Voltammetry	Urine	$0.4\,\mu M\,L^{-1}$	93.6–106	Present work

a) Capillary electrophoresis. b) Liquid-phase microextraction. c) High-performance liquid chromatography. d) Molecularly imprinted polymer. e) Sequential injection analysis. f) Differential pulse voltammetry.

This research work was sponsored by Council of Scientific & Industrial Research New Delhi (India) wide grant No. 01(2264)/08/EMR-II.

References

1 P. J. Kulesza, Z. Galus, *J. Electroanal. Chem.* **1992**, *323*, 261.
2 S. Sinha, B. D. Humphrey, A. B. Bocarsly, *Inorg. Chem.* **1984**, *23*, 203.
3 S.-M. Chen, M.-F. Lu, K.-C. Lin, *J. Electroanal. Chem.* **2005**, *579*, 163.
4 T. A. Denisova, L. G. Maksimova, D. G. Kellerman, M. A. Melkozerova, E. V. Zabolotskaya, V. Ya. Mitrofanov, G. A. Dorogina, *Solid State Phenom.* **2011**, *168–169*, 169.
5 J. Balmaseda, E. Reguera, A. Gómez, B. Díaz, M. Autie, *Microporous Mesoporous Mater.* **2002**, *54*, 285.
6 M. Avila, L. Reguera, J. Rodríguez-Hernández, J. Balmaseda, E. Reguera, *J. Solid State Chem.* **2008**, *181*, 2899.
7 J. Rodríguez-Hernández, E. Reguera, E. Lima, J. Balmaseda, R. Martínez-García, H. Yee-Madeira, *J. Phys. Chem. Solids* **2007**, *68*, 1630.
8 M. Yang, J. Jiang, Y. Yang, X. Chen, G. Shen, R. Yu, *Biosens. Bioelectron.* **2006**, *21*, 1791.
9 X. Cui, L. Hong, X. Lin, *J. Electroanal. Chem.* **2002**, *526*, 115.
10 Y. Shi, B. Zhou, P. Wu, K. Wang, C. Cai, *J. Electroanal. Chem.* **2007**, *611*, 1.
11 S.-M. Chen, K.-T. Peng, *J. Electroanal. Chem.* **2003**, *547*, 179.
12 S.-M. Chen, C.-M. Chan, *J. Electroanal. Chem.* **2003**, *543*, 161.
13 F. Qu, M. Yang, Y. Lu, G. Shen, R. Yu, *Anal. Bioanal. Chem.* **2006**, *386*, 228.
14 S. J. R. Prabakar, S. S. Narayanan, *Talanta* **2007**, *72*, 1818.
15 H. Razmi, A. Taghvimi, *Int. J. Electrochem. Sci.* **2010**, *5*, 751.
16 A. Eftekhari, *J. Electroanal. Chem.* **2002**, *537*, 59.
17 H. Heli, S. Majdi, N. Sattarahmady, A. Parsaei, *J. Solid State Electrochem.* **2010**, *14*, 1637.
18 P. Prabhu, R. S. Babu, S. S. Narayanan, *Sens. Actuators, B* **2011**, *156*, 606.
19 S. Boopathi, S. S. Kumar, J. Joseph, K. L. Phani, *Electrochem. Commun.* **2011**, *13*, 294.
20 K. K. Kasem, D. Hanninger, A. Croxford, F. Phetteplace, *Mater. Sci.-Pol.* **2010**, *28*, 439.
21 E. Bustos, L. A. Godínez, *Int. J. Electrochem. Sci.* **2011**, *6*, 1.
22 S.-F. Hong, L.-C. Chen, *Electrochim. Acta* **2010**, *55*, 3966.
23 F. Xu, M. Gao, L. Wang, T. Zhou, L. Jin, J. Jin, *Talanta* **2002**, *58*, 427.
24 M. Yamada, T. Sato, M. Miyake, Y. Kobayashi, *J. Colloid Interface Sci.* **2007**, *315*, 369.
25 S. P. Moulik, G. C. De, A. K. Panda, B. B. Bhowmik, A. R. Das, *Langmuir* **1999**, *15*, 8361.
26 N. Bagkar, R. Ganguly, S. Choudhury, P. A. Hassan, S. Sawant, J. V. Yakhmi, *J. Mater. Chem.* **2004**, *14*, 1430.
27 A. P. Baioni, M. Vidotti, P. A. Fiorito, S. I. C. de Torresi, *J. Electroanal. Chem.* **2008**, *622*, 219.
28 M. Yang, Y. Yang, F. Qu, Y. Lu, G. Shen, R. Yu, *Anal. Chim. Acta* **2006**, *571*, 211.
29 M. Ocaña, M. P. Morales, C. J. Serna, *J. Colloid Interface Sci.* **1999**, *212*, 317.
30 M. Cao, X. Wu, X. He, C. Hu, *Chem. Commun.* **2005**, 2241.
31 S. R. Ali, V. K. Bansal, A. A. Khan, S. K. Jain, M. A. Ansari, *J. Mol. Catal. A: Chem.* **2009**, *303*, 60.
32 F. Li, J. Song, D. Gao, Q. Zhang, D. Han, L. Niu, *Talanta* **2009**, *79*, 845.
33 M. H. Pournaghi-Azar, A. Saadatirad, *J. Electroanal. Chem.* **2008**, *624*, 293.
34 F. Li, J. Song, C. Shan, D. Gao, X. Xu, L. Niu, *Biosens. Bioelectron.* **2010**, *25*, 1408.
35 J. Dolezal, V. Kourim, *Radiochem. Radioanal. Lett.* **1969**, *1*, 295.
36 D. F. Shriver, *Struct. Bonding* **1966**, *1*, 32.
37 A. Ludi, H. U. Güdel, *Struct. Bonding* **1973**, *14*, 1.
38 P. J. Kulesza, M. A. Malik, M. Berrettoni, M. Giorgetti, S. Zamponi, R. Schmidt, R. Marassi, *J. Phys. Chem. B* **1998**, *102*, 1870.
39 C. A. Lundgren, R. W. Murray, *Inorg. Chem.* **1988**, *27*, 933.
40 Q.-L. Zhang, J.-J. Xu, X.-Y. Li, H.-Z. Lian, H.-Y. Chen, *J. Pharm. Biomed. Anal.* **2007**, *43*, 237.
41 Z. Zhang, C. Zhang, X. Su, M. Ma, B. Chen, S. Yao, *Anal. Chim. Acta* **2008**, *621*, 185.
42 W.-M. Yeh, K.-C. Ho, *Anal. Chim. Acta* **2005**, *542*, 76.
43 K.-C. Ho, W.-M. Yeh, T.-S. Tung, J.-Y. Liao, *Anal. Chim. Acta* **2005**, *542*, 90.
44 A. M. Idris, A. O. Alnajjar, *Talanta* **2008**, *77*, 522.
45 A. Niazi, J. Ghasemi, M. Zendehdel, *Talanta* **2007**, *74*, 247.
46 A. Salimi, R. Hallaj, G.-R. Khayatian, *Electroanalysis* **2005**, *17*, 873.